

A novel combined-design of an antenna-filter RF with optical anisotropy of nematic liquid crystal for UWB applications

SAYED MISSAOUI*, MOHSEN KADDOUR^a

LR99ES16 Physics Laboratory of Soft Matter and Electromagnetic Modeling, University of Tunis Elmanar, Faculty of Science of Tunisia, 2092, Tunisia

UR16ES03 Research Unit Advanced Materials and Nanotechnologies, University of Kairouan, Higher Institute of Applied Sciences and Technology of Kasserine, Department of Technology, Tunisia

^aUniversity of Sfax, Faculty of Science of Sfax, Department of Physics, Tunisia

We propose and demonstrate novel reconfigurable combined design (co-design) of an antenna-filter radio frequency (RF) with optical anisotropy of nematic liquid crystal (NLC). The basic co-antenna-filter is designed using microstrip interdigital coupled lines at the middle of the common ground plane. For these devices, reconfigurable Ultra-Wide Band (UWB) co-design has gained tremendous research interest for many different applications, cellular radio system, radar system and satellite communications. A reshaped structure with a NLC cavity has been used in order to improve the device performance, miniaturization and defined as its capacity to change the fundamental properties. Liquid Crystal (LC) decrease the return loss and VSWR of the co-design antenna-filter and 44% frequency agility is obtained.

(Received June 10, 2018; accepted April 8, 2019)

Keywords: Nematic Liquid Crystals, Optical Anisotropy, UWB-Antenna, Microwave Filter, Reconfigurable design

1. Introduction

With the rapid extension of wireless communication systems, reconfigurable antenna and filter technologies have received substantial consideration in the communications world. The reconfigurable antenna commonly adapts its properties to achieve operation in several frequency bands or change frequency for several services while maintaining desired radiation characteristics. The demand on tunable or reconfigurable components at micro- and millimeter waves increased during the last years. Today, these difficult problems are the subject of intensive studies in microwave planar filters [1–4].

For such applications, the use of combined antenna-filter appears as a quite convenient solution based on cascaded technique is used to reduce the cost and the overall volume of RF front-end subsystem especially in wireless communication systems. The agile microwaves devices [5–7] permit a compensation of the technological scatterings, the improvement of the instrumentation and the increase of the integration functions [8–11].

An alternative method for frequency reconfiguration is provided by material variation. Generally in this technique, an applied static electric field is used to change the relative permittivity of a material embedded in the

devices. These changes in relative permittivity can result in frequency shifting [12–13].

Reconfigurability with tuneable material is a very new research area and still facing challenges such as reliability, efficiency and proper modelling. However, in recent times many researches are carried out in this area and notable achievements have been reported [14–16]. Another approach which has recently gained some research interest is the liquid crystals (LCs) tuneable antennas. LC is essential materials for the scientific and industrial progress of the electro-optic display technology it is a group of organic molecules that show a set of peculiar properties. One property is that an LC molecule is polarisability depends on its orientation with respect to the electric (or magnetic) field. When an RF field orientation is imposed by the wave-guide, the LC has an effective permittivity that is seen by the RF field. So, in changing the LC's orientation, this permittivity can be changed and thus the electric length of the device and the wave travels faster or slower depending on your bias field.

The permittivity of a liquid crystal can be varied with DC bias voltage. LC state is known to vary with temperature from solid to liquid. The nematic phase corresponds to the state where molecules have an orientational order, but no positional one. Application of an electric field to LC changes the direction of molecules and may create significant anisotropy, which explains why

LC is currently chosen for microwave applications. This optical anisotropy varies with frequency and temperature [17].

In this paper, a new technique to reduce the cost and the overall volume of RF front-end subsystem especially in wireless communication systems, to minimize the processing power required to analyze the signals acquired by reconfigurable UWB-antenna and enhance the performance of the combined filter-antenna, is proposed. The idea is based on producing radiating and filtering system in a single device by integrating and matching a reconfigurable microwave filter within the tunable UWB-antenna structure using multi-layer technology. The frequency tuning of the combined structure is ensured by the use of LC material.

2. Nematic LC properties in the microwave range

In order to describe the operating mode of the agile tunableco-design, the microwave property of the LC is presented. The main property of the LC in the microwave range is the dielectric anisotropy due to the application of a static electric or magnetic field. All further explanations are related to nematic LCs, which have so far shown the best dielectric properties at microwave and mm-wave frequencies. The nematic phase is the most commonly used phase of LCs, especially at microwave and millimeter wave frequency. In this phase of liquid, through applying an external bias voltage, the electric field in the LC affects the orientation of the molecules [18]. At low voltage the effect is slight but it increases as the voltage increases. When the applied voltage reaches a certain level, all molecules are orientated stably along the direction of the electric field. LC is specified by different phases depending on their temperature. These phases determine the state of the material, which can vary from a solid state to a liquid state. In this study, LC is used in the nematic phase, where the molecules float around as in the liquid phase but are still ordered in their orientation. The nematic phase [19-22] is of great interest because of the dielectric anisotropy that permits the frequency agility [23].

In the following we assume the following law for the orientation angle (the angle of the director with respect to the x axis): $\theta=0$ for $V \leq V_c$, and $\theta = \pi/2 - 2 \arctan \exp(-(V-V_c)/V_0)$ for $V > V_c$, with $V_c = 1V$ and $V_0 = 2V$ [24]. We thus get the following expression of the permittivity matrix as a function of the orientation angle θ :

$$\varepsilon = \begin{pmatrix} \varepsilon_{1,1} & 0 & \varepsilon_{1,3} \\ 0 & \varepsilon_{\perp} & 0 \\ \varepsilon_{3,1} & 0 & \varepsilon_{3,3} \end{pmatrix} \quad (1)$$

$$\varepsilon_{1,1} = \varepsilon_{//} \cos^2(\theta) + \varepsilon_{\perp} \sin^2(\theta),$$

$$\varepsilon_{3,3} = \varepsilon_{\perp} \cos^2(\theta) + \varepsilon_{//} \sin^2(\theta),$$

$$\varepsilon_{1,3} = \varepsilon_{3,1} = (\varepsilon_{//} - \varepsilon_{\perp}) \cos(\theta) \sin(\theta).$$

Liquid crystals are uniaxial, due to their shape and polarization anisotropy, and are therefore anisotropic optic (birefringence), exhibiting different properties for light traveling with the electric field propagating parallel and perpendicular to the director or optic axis. Optical anisotropy is then defined as the difference between parallel and perpendicular permittivities and ensues from the following relation:

$$\Delta\varepsilon = \varepsilon_{//} - \varepsilon_{\perp} \quad (2)$$

where $\varepsilon_{//}$ and ε_{\perp} are, respectively, the parallel and perpendicular relative dielectric permittivity. The optical anisotropy is:

$$\Delta\varepsilon = \frac{N h f S}{\varepsilon_0} \left[\Delta\alpha + \frac{\mu^2 f}{2 K T} (3 \cos^2 \beta - 1) \right] \quad (3)$$

Where N is the number density, h is the reaction field, f is the reaction cavity parameters, S is the order parameter, $\Delta\alpha$ is the anisotropy in polarizability, μ is the molecular dipole moment, K is the Boltzmann constant, T is the temperature and β is the angle with molecular axis.

The electric field of the ordinary-ray is always perpendicular to the optic axis, so its refractive index n_o is a constant independent of propagation direction. The electric field of the extraordinary-ray lies in a plane that contains the optic axis, so its refractive index $n_e(\theta)$ varies with the ray propagation angle θ with respect to the optic axis according to

$$n_e(\theta)^2 = \left(\frac{\cos^2 \theta}{n_o^2} + \frac{\sin^2 \theta}{n_e^2} \right)^{-1} \quad (4)$$

This relationship is illustrated by the refractive index ellipsoid shown in Fig. 1. The birefringence of the medium, $\Delta n(\theta)$, depends on the propagation direction and is defined as

$$\Delta n(\theta) = n_e(\theta) - n_o \quad (5)$$

where $n_e = n_e(\theta = 90^\circ)$. Δn is defined as the difference between there fractive indices for the o- and the e-rays of a fully oriented nematic phase [25] propagating parallel and orthogonal, respectively, to the optic axis of the nematic medium.

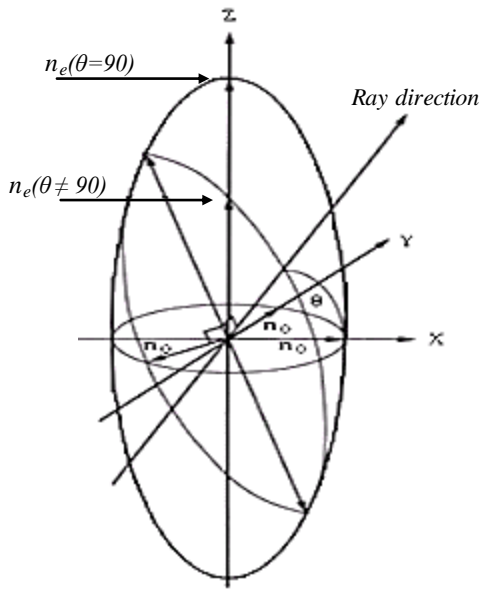


Fig. 1. The refractive index ellipsoid of a uniaxial LC phase with the optic axis parallel to the x axis. The refractive index n_o of the ordinary ray is independent of propagation. The refractive index n_e of the extraordinary ray is larger than n_o for a LC material of positive birefringence [26]

The order parameter is the degree to which the individual molecules align with the average direction. It is defined in terms of the angle that the molecules make with \vec{n} , the vector describing the average direction.

For values of the angle $\theta < 54.7^\circ$, the dipolar term is positive, and for values $\theta > 54.7^\circ$, the dipolar term is negative, and may result in a materials with an overall $-\Delta\epsilon$.

The dielectric permittivity ϵ of a material is defined as the ratio of the capacitance C_{mat} of the parallel plate capacitor that contains the material to the capacitance C_{vac} of the same capacitor that contains a vacuum:

$$\frac{C_{mat}}{C_{vac}} = \epsilon \tag{6}$$

The dielectric constants are dependent on the temperature and the frequency of the applied field up to the transition to the isotropic liquid. Fig. 2(a) shows a nematic-to-isotropic phase transition temperature, LC can exist in two phases. In one phase, the molecules tend to all line up; this is called the nematic phase. At high enough temperatures, however, this crystalline phase disassociates into an isotropic phase where the molecules have no preferred orientation. Fig. 2(b) shows the optical micrograph of the characteristic Schlieren texture, Nematic phases can be identified using optical polarising microscopy by two and four point defects in the resulting "Schlieren" texture.

Figs. 3 and 4 have shown the chemical structure and the molecular arrangements of 5CB LC in different phase states. The director vector \vec{n} has the same direction as the nematic LC molecules. A parallel permittivity $\epsilon_{||}$ of the molecules occurs for a microwave field parallel to the director \vec{n} , whereas a perpendicular permittivity ϵ_{\perp} is effective for a microwave field perpendicular to the director \vec{n} . The result of applying a sufficiently large control voltage to LC is to align the LC along the electric field due to the control voltage. This LC alignment is nearly parallel to the microwave electric field because the transmission mode of the Microstrip line is quasi-TEM. On the other hand, if the control voltage is removed (changed to 0 V), the LC becomes aligned in the direction determined by the alignment layers, which is perpendicular to the microwave electric field.

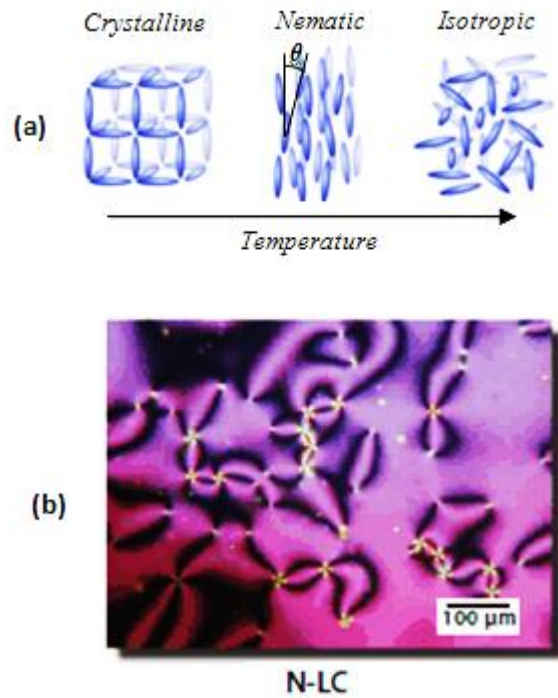


Fig. 2. LC Properties: (a) a nematic-to-isotropic phase transition temperature, (b) Schlieren texture for nematic LC is observed in polarized optical microscope

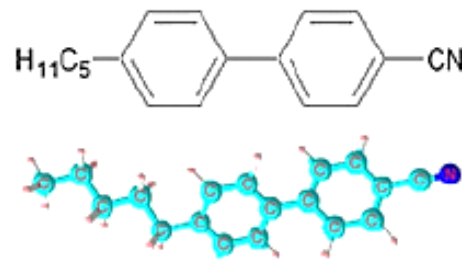


Fig. 3. Chemical structure of nematic liquid crystal 5CB

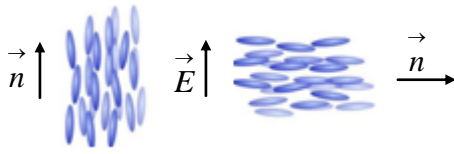


Fig. 4. Configuration matching the nematic permittivity $\epsilon_{//}$ and ϵ_{\perp}

3. UWB-antenna design and simulated results

The tuneable UWB-antennas have become attractive candidates in the present day communication systems due to their size that is smaller than the size of a conventional L-shaped strip and to their low profile, conformable to planar and non-planar surfaces, simple and inexpensive to manufacture using modern printed-circuit technology. In the designing process of UWB-antenna, which offers the advantage of ease of integration with active devices due to their uniplanar design and eliminating the need for vias, we have to first specify the operating resonant frequency f , the permittivity of the dielectric substrate material ϵ_r and the thickness of the substrate h . Then the width (W) of the microstrip patch antenna is calculated by [9].

$$W = \frac{c}{2f_c} \sqrt{\frac{2}{\epsilon_r + 1}} \quad (7)$$

where f_c is the centre frequency and ϵ_r is the relative permeability of the substrate material. ΔL and ϵ_{reff} is respectively extended incremental length and efficient permittivity of the patch can be calculated using the equations given below [26]:

$$\frac{\Delta L}{h} = 0.412 \frac{(\epsilon_{reff} + 0.3) \left(\frac{W}{h} + 0.264 \right)}{(\epsilon_{reff} - 0.258) \left(\frac{W}{h} + 0.8 \right)} \quad (8)$$

$$\epsilon_{reff} = \frac{\epsilon_r + 1}{2} + \frac{\epsilon_r - 1}{2} \left[1 + 12 \left(\frac{h}{W} \right) \right]^{-\frac{1}{2}} \quad (9)$$

The effective length can be calculated by the following equation:

$$L_{eff} = \frac{c}{2f_c \sqrt{\epsilon_{reff}}} \quad (10)$$

The actual length of patch can be calculated by the following equation:

$$L = L_{eff} - 2\Delta L \quad (11)$$

Microstrip antenna design using above equations “4 to 8” has attractive features such as light weight, conformability and low cost. However, major disadvantage of patch antenna is narrow bandwidth. But, there are many techniques to overcome this problem and convert the microstrip antenna into UWB such as increasing the height of the substrate, adding a step beneath the patch, using partial ground [27], using of tuning stub and notches [28].

The UWB-antenna is modeled numerically by using a commercially available simulation tool (HFSS software) based on Finite-Element-Method (FEM) in order to evaluate the electric overall performance. Parametric study for different parameters of the antenna has been performed to find the most optimum values.

Fig. 5 shows the top side design of a compact UWB-antenna. We have designed the proposed configurable UWB-antenna using rectangular radiation patch with notches and composed of an L-shaped microstrip line which is capacitively coupled to a small feeding line. This antenna is printed on bottom layer of a Rogers 5880 substrate (permittivity $\epsilon_r=2.2$, loss tangent $\tan\delta=0.0009$), having a thickness of $h = 1.575 \text{ mm}$. The L-shape strip is capacitively coupled to the small feeding line via an air gap, the length is 35.7 mm and the slot gap is 0.85 mm wide. The length of the L-shaped strip determines the operating frequency (2.4 GHz) of the antenna. The ground plane covers the back side of the substrate with a size of $25 \times 40 \text{ mm}^2$. Ground plane or metal cavity is often used to achieve directional radiation from an omni-directional antenna element. The effect of a ground plane can be seen as a short circuited transmission line connected to the antenna. The UWB-antenna is designed to match 50Ω characteristic impedance. The impedance matching of the proposed antenna is enhanced by correctly adjusting the dimension of the feeding structure and the radiating patch size and the whole structure is backed by a conducting metal ground plane.

The design dimension has been optimized in order to match over a frequency range of 1 GHz to 10 GHz and has resonant frequency at 2.4 GHz. By optimizing the L-shaped microstrip line and notch attached to the rectangular radiation patch, improved impedance bandwidth performance can be achieved for the proposed antenna.

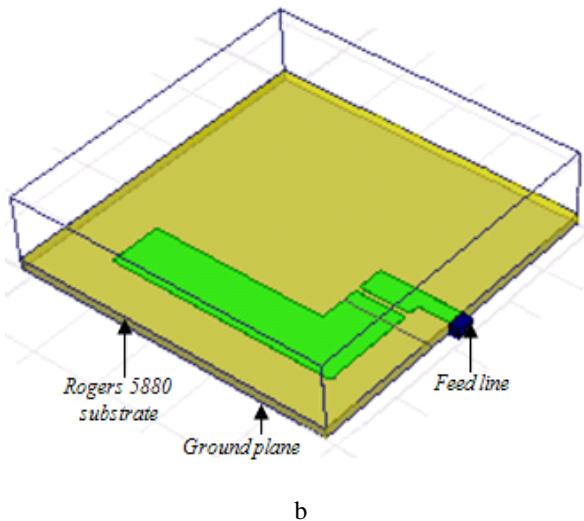
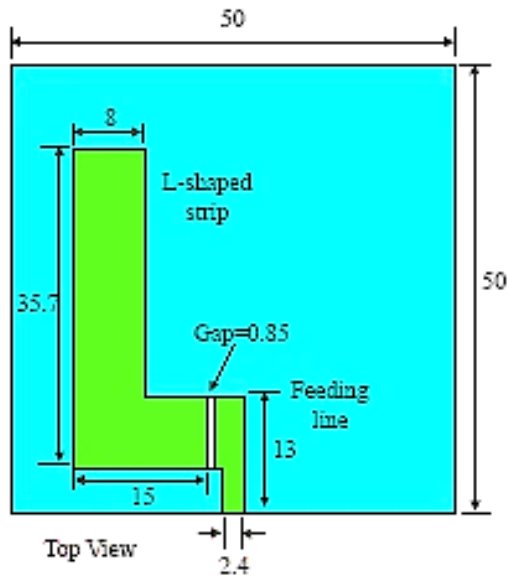


Fig. 5. (a) Dimensions of the UWB-antenna with L-shaped microstrip line, (b) Design of the UWB-antenna by (HFSS)

Fig. 6 depicts the results of simulated return loss, it can be observed that simulated return loss achieved -16 dB at 2.4 GHz. The bandwidths of the antenna are 100 MHz (4.16 %).

A two dimensional view of the far-field radiation patterns is presented in Fig. 7. Evidently, the UWB-antenna element possesses a wide beam width. The half power beam width at 2.4 GHz is more than 65° along E-plane (yz-plane) while the front-to-back ratio (FBR) is better than 16dB. The back radiation can be further reduced by increasing the ground plane size. We can conclude that while polarization is extremely pure in the E plane ($\phi=90^\circ$). From the Fig. 8, it is clearly seen that the simulated VSWR of UWB-antenna achieved 2.5 at the 2.4 GHz.

A new integration technique of a reconfigurable filter and antenna is proposed which allows the antenna to connect directly to the filter without any matching circuits.

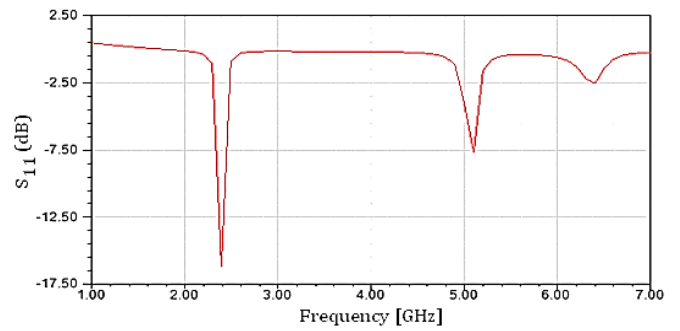


Fig. 6. Simulated return losses without LC

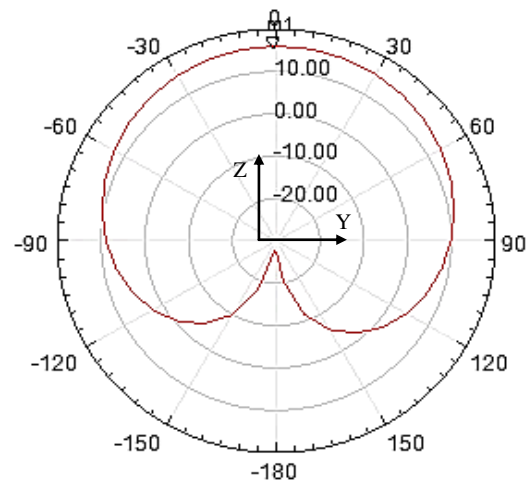


Fig. 7. Simulated radiation patterns for E plane ($\phi=90^\circ$) at 2.4 GHz

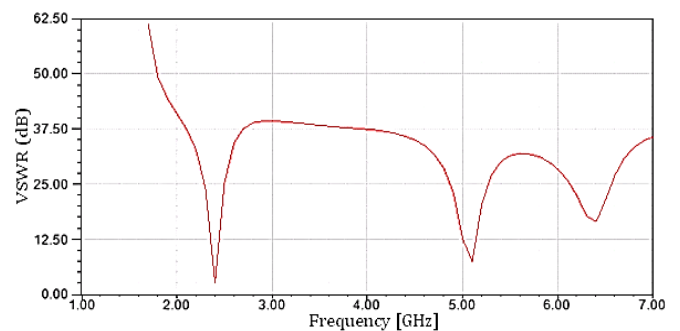


Fig. 8. Simulated VSWR

4. Reconfigurable integrated filter and UWB-antenna design and results

To minimize the loss and increase the gain, a new combined structure has been proposed. A basic structure of an integrated microwave filter and UWB-antenna in a multilayer structure was chosen to demonstrate the concept, which designed using microstrip interdigital coupled lines. The design of the proposed novel integrated microwave filter and UWB-antenna with L-shaped microstrip line based on LC is shown in Fig. 9. From the simulation, it is found that the two main factors determine

the coupling between the filter and antenna are the position and the size of the L-shaped microstrip line at the Rogers 5880 substrate. Based on EM simulations and in order to achieve a better response, the antenna has to be shifted or off-set from the origin to critically couple between the filter and antenna with the L-shaped has localized on Rogers 5880 substrate.

It can be seen from Fig. 10 that the return loss without LC simulated achieved -100 dB, -96 dB and -82 dB respectively, to 3.6 GHz, 6.7 GHz and 9.2 GHz. The simulated return loss with LC achieved -107.5 dB, -100 dB and -102.5 dB respectively, to 2.5 GHz, 6.2GHz and 9.9 GHz. We noticed that the use of the LC decrease the return loss of the co-design antenna-filter of a values of -7.5 dB, -4 dB and -20.5 dB. The resonance frequency variation (ΔFr) with and without LC is 1100 MHz corresponding to a frequency agility of 44%. For this frequency agility we can use several applications in the same standard by varying each time the permittivity of the liquid crystal by the control of an external field. This application are Mobile (GSM 900 MHz, DCS 1800 MHz, UMTS 2 GHz, LTE 800 MHz 2.6 GHz), WiFi/Bluetooth/UWB at 2.5 to 6 GHz, GPS 1.5 GHz, air surveillance military radars at 2 to 4 GHz and meteorological radars at 4 to 8 GHz.

The technique of microwave filter integration in an UWB antenna has also reduced the return loss by a value of -17.5 dB to a value of 107.5 dB, with the addition of liquid crystal in the combined structure, which is we gained 90 dB of insertion loss.

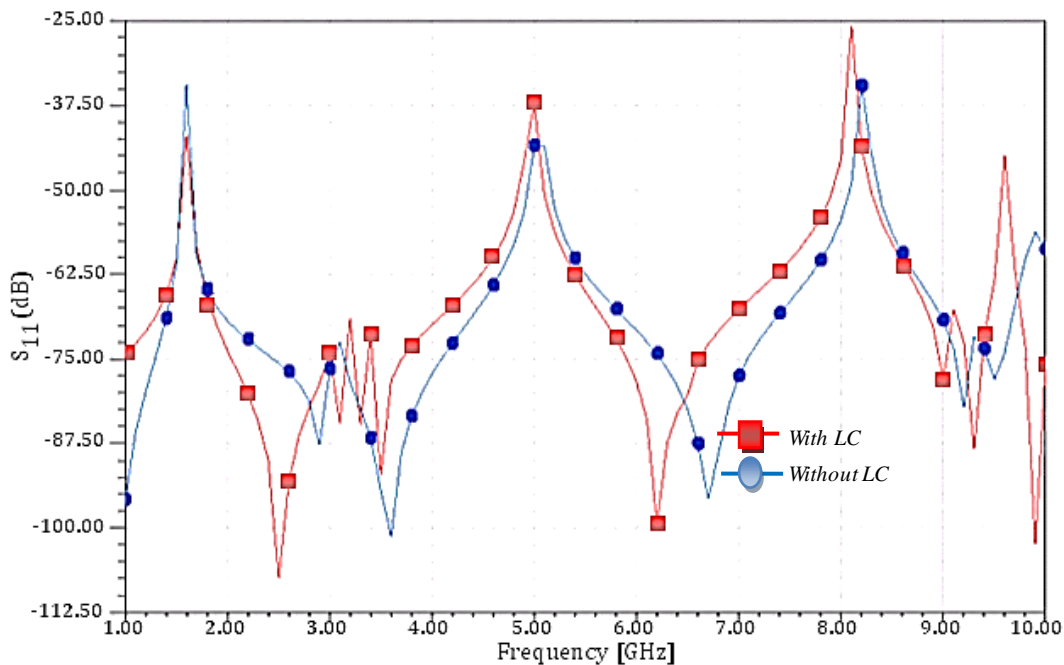


Fig. 10. Simulated return loss for co-design of an antenna-filter with and without LC

Fig. 11 depicts the simulated VSWR with and without LC for the reconfigurable integrated filter and antenna. It can be seen that the VSWR without LC equal to 1.038, 1.013 and 1.037 respectively, to 1.6 GHz, 5.1 GHz and 8.2 GHz. The VSWR results with LC equal to 1.004, 1.028 and 1.108 respectively, to 1.6 GHz, 5GHz and 8.1 GHz. We noticed that the use of the LC decrease the VSWR of the novel co-design antenna-filter of a value of 0.034 in the first band.

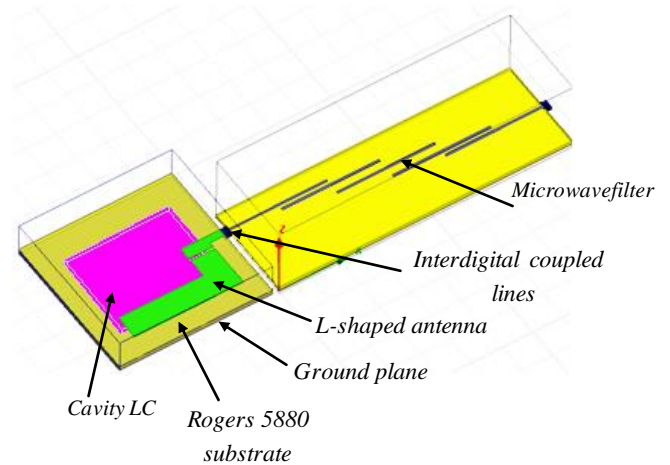


Fig. 9. Novel integrated microwave filter and UWB-antenna with L-shaped microstrip line based on LC

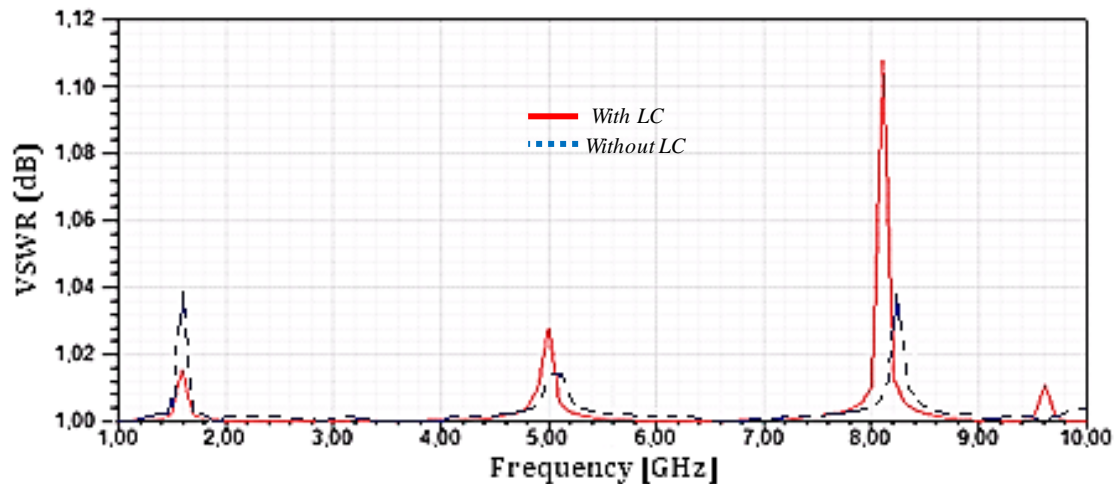


Fig. 11. Simulated VSWR with and without LCs

5. Conclusion

A novel tunable co-design filter and UWB-antenna for microwave front-end subsystems is proposed. The fundamentals of LC material and its application for combined structure are noted. The results confirmed the frequency agility by using LC dielectric permittivity with applied a low DC voltage, improved the radiation characteristics and decreased the return loss and VSWR of the device. This novel design provides an alternative solution for combining microwave filter and UWB-antenna to produce filtering and radiating element in a single reconfigurable module which can be useful in microwave RF front-end subsystems where the reduction of overall physical volume and cost and the improvement of the performances is a necessity.

References

- [1] H. Zhu, Q.-X. Chu, *IEEE Microw. Wireless Compon. Lett.* **23**(10), 572 (2013).
- [2] S. Fallahzadeh, M. Tayarani, *Journal of Electromagnetic Waves and Applications* **4**(7), 893 (2010).
- [3] Z.-C. Hao, S. Hong, *IEEE Trans. Microw. Theory Tech.* **58**(4), 941 (2010).
- [4] J. Xu, W. Wu, W. Kang, C. Miao, *IEEE Microw. Wireless Compon. Lett.* **22**(7), 351 (2012).
- [5] A. Petosa, *IEEE Antennas and Propagation Magazine* **54**, 271 (2012).
- [6] G. Perez-Palomino, P. Baine, R. Dickie et al., *IEEE Transactions on Antennas and Propagation* **61**, 1704 (2013).
- [7] P. Yaghmaee, C. Fumeaux, B. Bates, A. Manabe, O. H. Karabey, R. Jakoby, *Electronics Letters* **48**(12), 798 (2012).
- [8] V. Palazzari, D. Thompson, N. Papageorgiou et al., in *Proceedings of the IEEE 54th Electronic Components and Technology Conference Symposium (ECTC '04)*, 1658 (2004).
- [9] Z. Zakaria, W. Y. Sam, M. Z. A. Abd Aziz, K. Jusoff, M. A. Othman, B. H. Ahmad, M. A. Mutalib, S. Suhaimi, *Australian Journal of Basic and Applied Sciences* **7**(3), 24 (2013).
- [10] S. Missaoui, Sihem. Missaoui, Mohsen Kaddour, *European Journal of Scientific Research* **120**(2), 153 (2014).
- [11] A. Pal, H. Zhou, A. Mehta, *Radio and Wireless Symposium (RWS)*, IEEE, (2017).
- [12] S. Missaoui, M. Kaddour, *Electromagnetics* **38**(8), 489 (2018).
- [13] N. Martin, G. Prigent, P. Laurent, P. H. Gelin, F. Huret, *Microwave and Optical Technology Letters* **43**(4), 338 (2004).
- [14] K. Wang, S. W. Wong, Q. X. Chu, *Microw. Opt. Technol. Lett.* **55**(7), 1577 (2013).
- [15] M. Nosrati, M. Daneshmand, *IET Microw. Antennas Propag.* **8**(6), 862 (2012).
- [16] J.-D. Zhao, J.-P. Wang, G. Zhang, J.-L. Lin, *IEEE Microw. Wireless Compon. Lett.* **23**(12), 638 (2013).
- [17] S. Missaoui, S. Missaoui, M. Kaddour, *International Journal of Hydrogen Energy* **42**(13), 8804 (2017).
- [18] A. V. Zakharov, L. V. Mirantsev, *Phys Solid State* **45**(1), 183 (2003).
- [19] Sheng-Hua Lu, W. Chien-Yell, H. Cho-Yen, C. Kuan-Yu, C. Hui-Yu, *Applied Optics* **51**(9), 1361 (2012).
- [20] Xiaoxi Qiao, Xiangjun Zhang, Yanbao Guo, Shikuan Yang, Yu Tian, Yonggang Meng, *Rheol. Acta* **52**, 939 (2013).
- [21] N. Martin, P. Laurent, F. Huret, Ph. Gelin, *IEEE Trans. Microw. Theory Techniq. Long Beach (USA 2005)*.
- [22] B. Spinglart, N. Tentillier, F. Huret, C. Legrand, *Mol. Crystals Liquid Crystals* **368**, 183 (2001).
- [23] S. Missaoui, M. Kaddour, *Optoelectron. Adv. Mat.* **12**(1-2), 8 (2018).

- [24] T. S. Perova, V. A. Tolmachev, E. V. Astrova, Yu. A. Zharova, S. M. O'Neill, *Phys. Status Solidi C* **4**, 1961 (2007).
- [25] P. Chatelain, *Bull. Soc. Fr. Mineral Cristalog.* **77**, 353 (1954).
- [26] D. Demus, J. W. Goodby, G. W. Gray, H.-W. Spiess, V. Vill, Eds., "Physical Properties of Liquid Crystals," Wiley, New York, (1999).
- [27] Rajesh Kr. Raj, Sanjay Gurjar, Mayank Sharma, *International Journal of Computer Applications, National Seminar on Recent Advances in Wireless Networks and Communications, NWNC-2014* 22 (2014).
- [28] R. Sangeetha, B. Rajalakshmi, M. E. Notch, *International Journal of Computer Applications* **69**(9), 1 (2013).

*Corresponding author: sayed.elmissaoui@gmail.com